Int. J. Electrochem. Sci., 13 **(2018)** 7310 – 7320, doi: 10.20964/2018.08.46

International Journal of ELECTROCHEMICAL SCIENCE
www.electrochemsci.org

Traces of In^{3+} direct quantification by Anodic Stripping Differential Alternative Pulses Voltammetry in excess of Cd^{2+} and Pb^{2+}

Pablo Alberto Romero[1], *Roumen Zlatev*[1,*], *Margarita Stoytcheva*[1], *Velizar Gotchev*[2], *Benjamín Valdez*[1], *Gisela Montero*[1], *Roberto Ibarra*[1]

[1] Universidad Autónoma de Baja California, Instituto de Ingeniería, Blvd. Benito Juarez s/n, 21280 Mexicali B.C., Mexico
[2] Plovdiv University "P. Hilendarski", Faculty of Biology, Dep. Biochemistry and Microbiology, Plovdiv, Bulgaria
[*]E-mail: roumen@uabc.edu.mx

Received: 28 March 2018 / *Accepted:* 24 May 2018 / *Published:* 5 July 2018

The Differential Alternative Pulse Voltammetry (DAPV) was modified appropriately allowing its application in anodic stripping mode (ASDAPV). The modified technique parameters were optimized in terms of sensitivity and it was applied for direct species quantifications in industrial waste waters without sample pretreatment. Trace of In^{3+} was quantified *on-line* in presence of Cd^{2+} excess in industrial waste waters purified by *Streptomyces griseus* biomass loaded column. Reliable results for the In^{3+} concentration were obtained by the ASDAPV up to 11 fold excess of Cd^{2+} while peak overlapping occurs even at inferior Cd^{2+} concentration by the application in anodic stripping mode of the most commonly applied voltammetric technique, the DPV.

Keywords: Differential Alternative Pulse Voltammetry (DAPV), In^{3+} traces quantification, Stripping analysis

1. INTRODUCTION

The increased indium application in the semiconductor devices, touch screens, photovoltaics, etc. during the last few years caused corresponding augmentation of the industrial wastes containing this toxic heavy metal [1 - 3] and hence led to increased interest in its quantification. The most common laboratory analytical techniques as atomic adsorption spectrometry (AAS) and inductively coupled plasma (ICP) applied for indium quantification require sampling, samples conservation and transportation to equipped laboratories to be determined by trained personnel, making the analysis long

and cost ineffective [4, 5]. In contrast, the voltammetric techniques and especially the second order ones [6- 9] are very suitable for direct applications *on-site* because of their high resolution not requiring laboratory sample pretreatment, as well as because of the portable, simple and low cost equipment needed [6 - 33].

In case of trace concentrations measurement, the voltammetric technique have to be applied in stripping mode to obtain precise and reliable analytical results. Unfortunately, the resolution power of the second order voltammetric techniques applied in stripping mode degrades to that of the first order ones. Voltammogram shape altering occurs (anodic to cathodic peak ratio degradation), which makes problematic the peaks resolving. This problem defined the need of improvement of the second order voltammetric techniques allowing their application in stripping mode.

The second order voltammetric techniques are based on the nonlinearity of the I - E characteristic of the electrochemical systems resulting in its "electrochemical derivation" when periodic bipolar deviations (with rectangular or sinusoidal form and small amplitudes) are superimposed on the scanning DC potential [6-9]. The voltammogram's shape as second derivative of voltammetric wave combined with the small half-widths of the registered anodic and cathodic peaks for any of the quantified species allow their distinction in case of overlapping even at very small $E_{1/2}$ difference. Any of the anodic and the cathodic peaks belonging to different species remained on the voltammogram after the peaks overlapping can be employed for concentrations evaluation as showed the authors earlier [9]. Unfortunately, because of the negligible current response caused by the cathodic pulse in anodic stripping mode and the anodic one in cathodic stripping mode respectively, the voltammogram shape degrades to that of the first order voltammetric techniques (peak) annulling this way the second order techniques advantage in terms of resolution.

The most common interfering ions in case of In^{3+} voltammetric quantification are Cd^{2+}, Pb^{2+} and Sn^{2+} because of their very close $E_{1/2}$ potentials in almost all the supporting electrolytes [1]. Unfortunately, the interfering species concentrations are usually higher than that of In^{3+} which makes its precise voltammetric quantification problematic because of the peaks overlapping. For example, by the application of the first order technique Differential Pulse Voltammetry (DPV) peak overlapping occurs even at Cd^{2+} concentration less than that of In^{3+} (see the text below). Instrumental, mathematical and chemical approaches have been developed till now to solve the interference problem. The instrumental approach was directed mainly to the scan rate and the mercury film thickness optimization [1, 20, 34]. The chemical approach includes species extraction, complexation or inhibition requiring complicated sample pretreatment performed by trained personnel degrading the results precision and cost efficiency [18, 22, 35]. The mathematical approach applying digital methods for curve treatment is easy, but peak heights altering occurs causing quantification precision degradation [19]. Unfortunately, none of the mentioned approaches resulted in complete solution of the problem to yield precise quantification of In^{3+} traces in presence of higher concentrations of interfering species.

The Differential Alternative Pulse Voltammetry (DAPV) [9, 36] is a voltammetric technique introduced recently combining the simplicity and the high sensitivity of the Differential Pulse Voltammetry with the high resolution of the second order voltammetric techniques. Similar to the other second order techniques, the DAPV performance in stripping mode is inferior to its direct mode

in terms of resolution. The bipolar pulses application resulting in sharp anodic and cathodic peaks is the base of the DAPV high resolution, but on the other hand exactly the bipolar pulses application is the root of its resolution degradation in stripping mode. This led to the conclusion that to keep the DAPV high resolution when applied in stripping mode, same polarity pulses have to be applied combined with an appropriate signal processing yielding the specific DAPV voltammogram shape.

The objectives of this paper are: a) DAPV potential-time waveform and the signal processing modification allowing its application in anodic stripping mode (ASDAPV); b) ASDAPV parameters optimization for maximal resolution and sensitivity achievement; c) ASDAPV In^{3+} *on-line* monitoring in industrial waste waters containing excess of Cd^{2+} and Pb^{2+} purified by *Streptomyces griseus* [37] bacterial biomass loaded column.

2. EXPERIMENTAL

2.1. Instrumentation

EG&G PARC model 303A electrode stand in its original configuration was employed. Only in the real samples experiments its original glass cell was replaced by an acrylic homemade 5 mL flow type one. A small stream was diverted from the column flow controlled by a punch valve to fill acrylic cell and returned back to the column after the quantifications. Mercury was chosen as working electrode material because of its wide potential window allowing electrode potentials higher than -1V application in the deposition step of the ASDAPV. Mercury film electrodes were not preferred because of the HMDE easier surface renovation. The used mercury drops in the real samples experiments were separated by the gravity and collected in a flask before the sample returning to the column.

The reference electrode was Ag/AgCl/ KCl and a Pt wire served as auxiliary electrode, both part of the EG&G PAR 303A electrode stand. The samples were purged for 2 minutes with N_2 gas before the quantifications and 60 s deposition at -1.2 V was applied in all the experiments.

Model CompactStat.h 20250 potentiostat (Ivium Technologies, Netherlands) was used for the ASDAPV voltammograms registration by IviumPulse software application. The Hg drop change in HMDE mode, purging and stirring functions of the EG&G 303A electrode stand as well as the punch valve opening and closing were controlled by this software as well driven through the DB37 potentiostat peripheral port using a special homemade interface.

2.2. Reagents and supporting electrolytes

HCl (0.1 mol L^{-1}) was used as supporting electrolyte in all the experiment. No additional reagents to serve as supporting electrolytes were added in real samples experiments because the analyzed samples were returned back to the sorption column. For the ASDAPV characterization model solution using standard metal ions solutions of 1000 μg mL^{-1} (ULTRAgradeTM Solution from ULTRA Scientific, USA) of analytical grade were used.

3. RESULTS AND DISCUSSION

3.1. Potential-Time waveform and the signal processing modification

The DAPV potential-time waveform diagram was modified as presented in the first part of this work and according to the consideration mentioned above (see Figure 1). Unlike the original version of the DAPV potential-time diagram where one anodic and one cathodic pulse with a delay time between them were applied in the repetitive cycle [9] here the two pulses have the same polarity (anodic) and the delay time between them is zero. In case of cathodic stripping mode both pulses have to have cathodic polarity respectively.

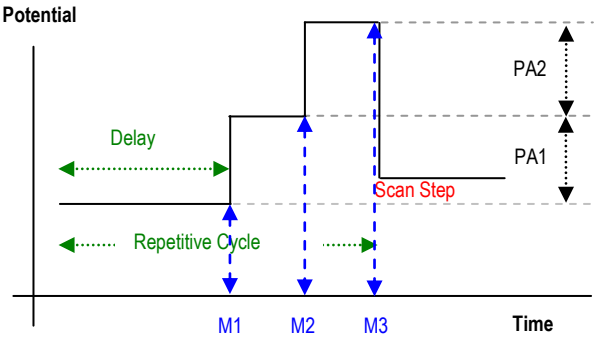

Figure 1. Potential-Time waveform of ASDAPV/CSDAPV: PA1 and PA2 are the pulse amplitudes and M1, M2, M3 are the measured currents responses.

The signal processing was modified as follows: the first pulse faradic current response M2 serves as a base value in the ASDAPV current response ΔI evaluation. In respect to this base value the first pulse can be considered cathodic, while the second one, anodic (see Figure 1):

$$\Delta Ip = M1 + M3 - 2M2 \quad (1)$$

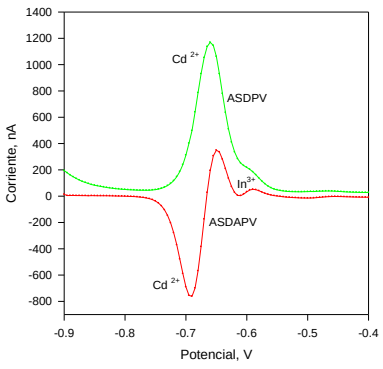

Figure 2. ASDAPV and ASDPV curves of 20 ppb In^{3+} and 160 ppb Cd^{2+} in 0.1 mol L^{-1} HCl registered at the same conditions. Deposition time = 60 s, PA1 = PA2 = 25 mV.

The timing was synchronized with the power line frequency of 60 (50) Hz as well as signal integration was performed for a full power line cycle period to reduce the electrical noise at the current

measurement. The optimal values determined experimentally and employed in all the ASDAPV experiments (see the text bellow) were as follows: the pulse widths were 33.3 ms (2 power line cycles) with integration time at the current measurement of 16.6 ms (1 power line cycle) at the ends of each pulse; a delay time of 200 ms (12 power line cycles) was applied between the scan step of 5 mV and the first pulse rising edge. The pulse amplitudes PA1 and PA2 were of +25 mV each.

A typical ASDAPV curve registered by the application of the modified potential – time waveform diagram, the modified signal processing and the mentioned optimal parameters values is presented in Figure 2 in comparison with the corresponding ASDPV curve registered at the same conditions. Separate and free of overlapping In^{3+} anodic peak and a Cd^{2+} cathodic peak appear on the ASDAPV curve while the In^{3+} peak is completely overlapped by that of Cd^{2+} on the ASDPV curve not allowing precise quantifications.

3.2. In^{3+} and interfering species $E_{1/2}$ determination

The $E_{1/2}$ of Cd^{2+} and Pb^{2+} are close to that of In^{3+} in all the supporting electrolytes applied for In^{3+} quantification: NaCl, HCl, $(NH_4)_2SO_4$, HNO_3, oxalic, citric, tartaric acids, KOH, LiOH, NH_4F, and HBr making the peaks resolving complicated [1].

According to the already published data [25] the $E_{1/2}$ difference between In^{3+} and Cd^{2+} is smaller than that with Pb^{2+} which turns the Cd^{2+} the most important interfering specie in case of In^{3+} quantification. The In^{3+}, Cd^{2+} and Pb^{2+} peak potentials were determined experimentally registering DPV curves in anodic stripping mode (ASDPV) of any of them separately at same conditions in supporting electrolyte of 0.1 mol L^{-1} HCl (see Figure 3).

$E_{peak\ Cd}$ = -0.675 V, $E_{peak\ In}$ = -0.630 V and $E_{peak\ Pb}$ = -0.475 V were determined from the voltammograms. Similar value for In^{3+}, Cd^{2+} and Pb^{2+} $E_{1/2}$ were also determined in KCl, NaCl and almost all the mentioned above supporting electrolytes applying the same procedure. Peaks overlapping occur on the ASDPV voltammograms at this small $E_{1/2}$ difference of 45 mV even at Cd^{2+} concentrations inferior to that of In^{3+}, as seen from Figure 3 right.

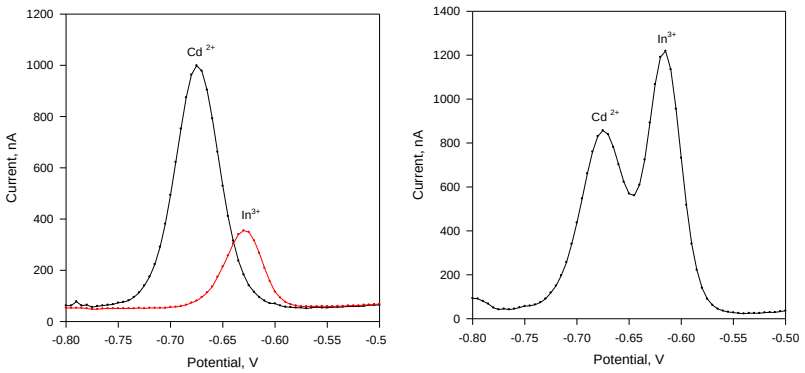

Figure 3. ASDPV curves registered on HMDE in 0.1 m L^{-1} HCl at pulse height of 25 mV, pulse width of 33.3 ms and deposition time of 60 s. Left: 35 ppb In^{3+} and 90 ppb Cd^{2+}. Right: 100 ppb of In^{3+} and 80 ppb of Cd^{2+}. The Pb^{2+} peak is not shown because of its much more positive $E_{1/2}$.

3.3. Pulse amplitudes ratio optimizing to obtain maximal ASDAPV resolution

The pulse amplitudes ratio variation alters the ASDAPV voltammogram shape changing the anodic to cathodic peak heights ratio affecting the ASDAPV resolution power as illustrated in Figure 4. Best Cd^{2+} and In^{3+} peaks resolving in case of superior Cd^{2+} concentration was achieved at PA2 = PA1 (see curve **b**).

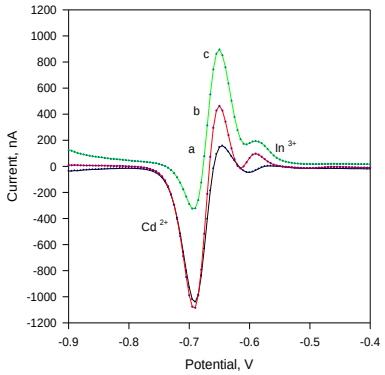

Figure 4. ASDAPV curves of 35 ppb Cd $^{2+}$ and 220 ppb In $^{3+}$ in 1 mol L-1 HCl, deposition time 60 s at -1.2 V. Pulse amplitudes for curve a: PA1 = 15, PA2 = 25 mV; for curve b: PA1 = PA2 = 25 mV; for curve c: PA1 = 25, PA2 = 15 mV

3.4. Pulses widths optimizing to obtain maximal ASDAPV sensitivity

The decay rate of the pulse faradaic current component determines the pulse width influence on the ASDAPV sensitivity as discussed in the first part of this work. ASDAPV curves of 60 ppb In^{3+} and 60 ppb Cd^{2+} in 0.1 mol L^{-1} HCl are shown in Figure 4 (left) registered with pulse widths of 2, 3, 4 and 5 power line periods of 16.66 ms. each.

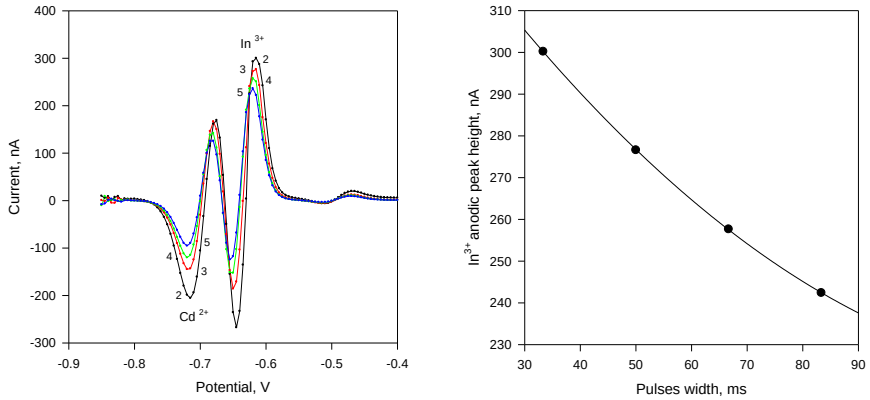

Figure 5. Left: ASDAPV curves of 60 ppb In^{3+} and 60 ppb Cd^{2+} in 0.1 mol L^{-1} HCl. Pulse width (2 to 5 power line cycles of 60 Hz = 33.33 to 83.33 ms). Deposition time = 60 s at -1.2 V. Right: In^{3+} peak heights as a function of the pulse width.

As seen in Fig. 5 maximal peak height (sensitivity0 can be obtain at pulse width equal to 33.3 ms or two power line cycles of 60 Hz.

3.5. Maximal Cd^{2+} to In^{3+} concentration ratio determination

Separate and overlapping free cathodic Cd^{2+} and anodic In^{3+} peaks appear on the ASDAPV voltammograms as presented in Figure 6. The right chart corresponds to In^{3+} concentration inferior than the Cd^{2+}, while the left chart illustrates the opposite case plus 1.6 times higher Cd^{2+} concentration.

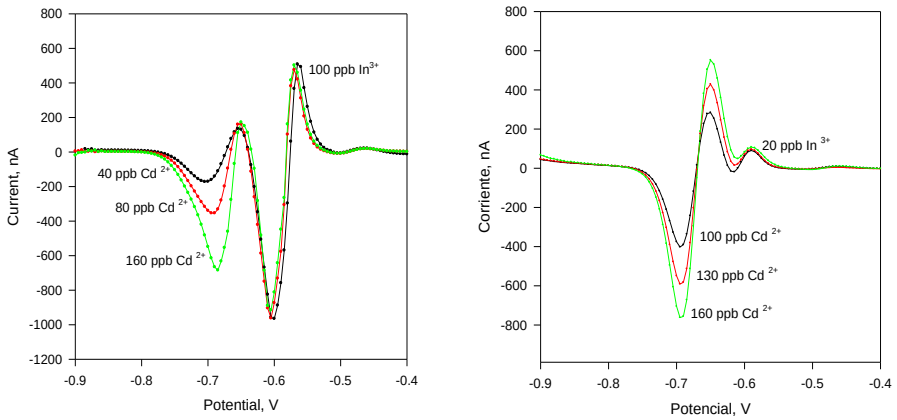

Figure 6. ASDAPV voltammograms at different concentration ratios of Cd^{2+} and In^{3+} in 0.1 mol L-1 HCl. Pulse amplitudes: PA1 = PA2 = 25mV. Deposition time = 60 s at -1,2 V.

In case of Cd^{2+} concentration superior to the one of In^{3+} the anodic Cd^{2+} peak base broadening with its concentration increase not affects at all the In^{3+} anodic peak up to Cd^{2+} to In^{3+} concentration ratio of 6 (see Figure 6 right). The further increase of this ratio up to 8 slightly alters the anodic In^{3+} peak and separate peaks are still registered up to ratio of 11 but affected by progressive overlapping. For comparison the Cd^{2+} and In^{3+} peaks are overlapped on the ASDPV curve even at ratio less than 1, as illustrated in Figure 3 right.

The shape, polarity and height of the resulting peak in the central part of the charts (see Figures 6 and 7) depend on the species concentrations ratio. In general this peak is not utilizable for analytical purpose.

3.6. Peaks half-width determination

The half-width of the peaks is the most important parameter determining the resolution power of any analytical technique. Smaller peak half-width allows avoiding peaks overlapping at simultaneous quantification of species having small $E_{1/2}$ difference or at their high concentration ratio. It is known that the voltammetric peak half-width depends on the pulse amplitude, lower the

amplitude, smaller the peak half-width and hence higher the resolution. However, low pulse amplitude leads to sensitivity decrease, so 25 mV was chosen as a balanced value for optimal sensitivity and resolution.

The Cd^{2+} and In^{3+} ASDAPV peak half-width values determined at PA1 = PA2 = 25 mV are presented in Table 1 in comparison with those obtained by ASDPV at the same conditions, determined from the curves presented in Figures 2 and 3. The data shown in the table fits well with those presented by the authors earlier related to the DAPV non-modified original version [9].

Table 1. ASDAPV and ASDPV $Cd^{2+}$and In^{3+} peaks half-widths

Voltammetric technique	In^{3+} peak half-width, mV	Cd^{3+} peak half-width, mV
ASDPV	38.8	48.4
ASDAPV	27.0	38.0
----------	ASDAPV/ASDPV half-width ratio = 0.69	ASDAPV/ASDPV half-width ratio = 0.78

3.7. ASDAPV characterization in terms of precision

The In^{3+} quantification precision in excess of Cd^{2+} was evaluated in the concentration ratio (Cd^{2+} to In^{3+}) from 0.4 up to 11 using the data derived from the voltammograms presented in Figure 6. Up to ratio of 6 the presence of Cd^{2+} practically does not affect the In^{3+} quantification and its precision equals to that of In^{3+} only quantification. Up to ratio of 11 the precision degrades progressively because of the peaks overlapping.

Table 2. Relative errors for In^{3+} quantification in presence of Cd^{2+}

Concentration ratio	6 or less	8	11
Relative error, % (5 assays)	+/- 1.72	-3.62	-5.23

3.8. ASDAPV application to real samples and results validation

Finally, the optimized ASDAPV pulse amplitudes and pulse widths values were applied for simultaneous In^{3+}, Cd^{2+} and Pb^{2+} real time monitoring in a *Streptomyces griseus* dead bacterial biomass loaded column used for metal uptake from industrial waste waters. HCl was preliminary added to the waste water for pH adjustment required by the sorption process and served as 0.1 mol L^{-1} supporting electrolyte as well. All the quantifications were performed directly without any sample pretreatment. The ASDAPV curves registered at the beginning and at the end of purification process is presented in Figure 8. The initial about 8-fold excess of Cd^{2+} (decreasing along the time) does not affect at all the In^{3+} quantification by ASDAPV allowing the precise simultaneous quantification of all the species.

The In^{3+}, Cd^{2+} and Pb^{2+} concentrations measured at the beginning of the purification process: 2.1 ppm, 15.9 ppm and 7.6 ppm respectively (see Figure 7 left) and their direct monitoring along the time by ASDAPV allow real time process control and purification column efficiency evaluation.

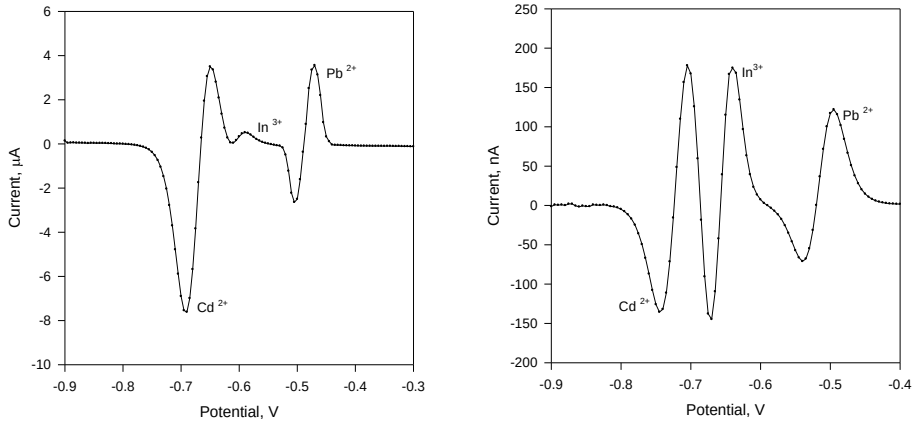

Figure 7. ASDAPV curve registered in industrial waste water at the beginning of the purification process (left) and at its end (right). PA1= PA2 = 25 mV, pulse width = 33.3 ms, deposition time = 60 s at -1.2 V, HMDE.

The In^{3+}, Cd^{2+} and Pb^{2+} trace concentrations obtained at the end of the purification process evaluated by ASDAPV application were validated by ICP in independent laboratory and the results are presented in Table 3. Preliminary build calibration curves in 0.1 mol L^{-1} HCl was employed for the concentrations evaluation by ASDAPV.

Table 3. In^{3+}, Cd^{2+} and Pb^{2+} concentrations at the end of the purification process comparison evaluated by ASDAPV and ICP

Analytical method	In^{3+}, ppb	Cd^{2+}, ppb	Pb^{2+}, ppb
ASDAPV	36.2	28.4	25.5
ICP	36.9	27.8	26.1
Rel. Error %	-1.89	2.15	-2.29

The results obtained for In^{3+} quantification in presence of excess of Cd^{2+} by ASDAPV were compared with data obtained by other methods reported in the literature. Geca et al [38] proposed a stripping procedure for In^{3+} determination by anodic stripping voltammetry using double deposition step on GC electrode and Bi film deposited on GC electrode in 0.1 mol L^{-1} acetate buffer (pH 4.5) and 0.1 mol L^{-1} KBr applied as supporting electrolytes. The $E_{1/2}$ difference of the two species is about 110 mV at these conditions, allowing the In^{3+} and Cd^{2+} peak resolving. The main drawback of this analytic procedure however is the very complicated manner of the electrode surface preparation making it hard to be applied in the analytical practice leading also to quantification precision degradation (RSD = 5.3 %).

Charalambous et al [24] reported Bi film electrode (BiFE) application for In^{3+} and Cd^{2+} simultaneous quantification in supporting electrolytes with different composition employing DPV.

Complete overlapping of the In^{3+} and Cd^{2+} peaks occurs in acetate buffer improved by the addition of KCl, KSCN and KBr. The main drawback of this method is the In^{3+} peak height dependence on the Bi^{3+} concentration added to the sample to form the BiFE, which strongly affects the quantification precision. The maximal In^{3+} to Cd^{2+} concertation ratio reported was 1 to 8 – 12. The ASDAPV results presented here showed that ASDAPV allows the achievement of same In^{3+} to Cd^{2+} concentration ratio applying much simpler and rapid procedure allowing its application in *on-line* analysis.

4. CONCLUSION

The potential-time waveform and signal processing of the second order voltammetric technique DAPV were modified which allowed its application in stripping mode. Parameters as pulses width and pulse amplitudes ratio were optimized to achieve maximal resolution and sensitivity. Precise In^{3+} quantification were obtained at Cd^{2+} to In^{3+} concentration ratio as high as 11:1 at 45 mV $E_{1/2}$ difference, while peaks overlapping occurs even at ratios less than 1:1 at the same conditions by the application of the commonly used voltammetric technique ASDPV. Finally, the improved voltammetric technique was applied for precise simultaneous *on-line* ASDAPV trace of In^{3+}, Cd^{2+} and Pb^{2+} quantification in industrial waste waters purified by *Streptomyces griseus* dead biomass loaded columns without any sample pretreatment.

ACKNOWLEDGEMENT
The publishing fees were funded by PFCE 2017 program to Universidad Autonoma de Baja California, Instituto de Ingenieria.

References

1. K. Honeychurch, *World Journal of Analytical Chemistry*, 1 (2013) 8.
2. Y. Nozaki, D. Lerche, D. S. Alibo, M. Tsutsumi, *Geochim. Cosmochim. Acta*, 64 (2000) 3975
3. P. Hoet, E. De Graef, B. Swennen, T. Seminck, Y. Yakoub, G. Deumer, V. Haufroid, D. Lison, *Toxicol. Lett.* 213 (2012) 122
4. S. White, H. Hemond, *Crit. Rev. Env. Sci. Tec.*, 42 (2012) 155.
5. J. Wang, in: Stripping Analysis: Principles, Instrumentation, and Application", VCH Publishers, Inc., Deerfield Beach, FL, USA, 1985.
6. G. Barker, *Analytica Chimica Acta*, 18 (1958) 118.
7. D. Saur, *Frezenius Z. Anal.Chem.*, 298 (1979) 128.
8. P. Delahay, M. Senda, C. H. Weis, *J. Amer. Chem. Soc.*, 83 (1960) 312.
9. R. Zlatev, M. Stoytcheva, B. Valdez, J-P. Magnin, P. Ozil, *Electrochem. Commun*., 8 (2006) 1699.
10. J. Aguilar, E. Rodriguez de San Miguel, J. Gyves, *Rev. Soc. Quím. Méx.*, 45 (2001) 17.
11. P. Farias, C. Martin, A. Ohara, J. Gold, *Anal. Chim. Acta*, 293 (1994) 29.
12. A. Benvidi, M. Ardakani, *Anal. Letters*, 42 (2009) 2430.
13. T. Florence, G. Batley, Y. Farrar, *Electroanal. Chem*., 56 (1974) 301.
14. A. Ciszewski, Z. Lukaszewski, *Anal. Chim. Acta*, 146 (1983) 51.
15. I. Paolicchi, O. Domınguez Renedo, M. Asunción Alonso Lomillo, M. Arcos Martínez, *Anal. Chim. Acta*, 511 (2004) 223.

16. L. Medvecký, J. Briančin, *Chem. Pap*., 58 (2004) 93.
17. K. Pratt, W. Koch, *Anal. Chim. Acta*, 215 (1988) 21.
18. T. Liu, D. Lai, J. Osterloh, *Anal. Chem.*, 69 (1997) 3539.
19. K. Wikiel, Z. Kublik, *J. Electroanal. Chem.*, 165 (1984) 71.
20. A. Nosal-Wiercinska, G. Dalmata, *Monatsh Chem.*, 140 (2009) 1421.
21. J. Labuda, M. Vanickova, *Anal. Chim. Acta*, 208 (1988) 219.
22. G. Batley, T. Florence, *Electroanal. Chem. Interfacial Electrochem.*, 55 (1974) 23.
23. M Ali Taher, *Talanta*, 52 (2000) 301.
24. A. Charalambous, A. Economou, *Anal. Chim. Acta*, 547 (2005) 53.
25. A. Bobrowski, M. Putek, J. Zarebski, *Electroanalysis*, 24 (2012) 1071.
26. J. L. Zhang, Y. J. Shan, J. Ma, L. Xie, X. Y. Du, *Sensor Lett.*, 7 (2009) 605.
27. L. Sopha-Baldrianova, E. Tesarova, S. Hocevar, L. Svancara, B. Ogorevc, K. Vytras, *Electrochim. Acta*, 55 (2010) 7929.
28. C. Xiang, Y. Zou, J. Xie, X. Fei. J. Li, *Anal. Lett*ers, 38 (2005) 2045.
29. I. Gecaz M. Korolczuk, *J. Electrochem. Soc.*, 164 (2017) 183.
30. R. Ouyang, L. Xu, H. Wen, P. Cao, P. Jia, T. Lei, X. Zhou, M. Tie, X. Fu, Y. Zhao, H. Chang, Y. Miao, *Int. J. Electrochem. Sci.*, 13 (2018) 1423, doi: 10.20964/2018.02.02
31. A. M. Ashrafi, K. Vytřas, *Int. J. Electrochem. Sci.*, 8 (2013) 2095
32. E. Nagles, V. Arancibia, R. Ríos, C. Rojas, Int. J. Electrochem. Sci., 7 (2012) 5521
33. O. A. Farghaly, R. S. Abdel Hameed, A-A. H. Abu-Nawwas, *Int. J. Electrochem. Sci.*, 9 (2014) 3287
34. H. N. Hassan, M. E. M. Hassouna, *Talanta* 46 (1998) 1195.
35. J. Opydo, *Anal. Chim. Acta*, 298 (1994) 99.
36. R. Zlatev, M. Stoytcheva, B. Valdez, *Electroanalysis*, 22 (2010) 1671.
37. S. Antony-Babu, M. Goodfellow, *Antonie van Leeuwenhoek*, 94 (2008) 581
38. I. Geca, M. Korolczuk, *Journal of The Electrochemical Society*, 164 (4) 2017 H183